A Communication and Localization Framework Suited for Nomadic Wireless Sensor Networks

Luca Bencini
Dept. of Innovation & Technology
T.T. Tecnosistemi S.p.A.
Via Rimini 5, 59100 Prato, Italy
Luca.Bencini@tecnosistemi.com

Stefano Maddio
Dept. of Electronics and Telecommunication
University of Florence
Via di Santa Marta 3, 50139 Florence, Italy
stefano.maddio@unifi.it

***Abstract*—In this paper, an energy efficient communication and localization framework able to manage the synchronization between nodes and to provide the localization of nomadic nodes within Nomadic Wireless Sensor Networks is presented. It is comprised of a MAC protocol based on sleep and active states and a novel localization algorithm based on Differential Direction of Arrival. Some numerical simulations was performed to show the low power consumption of the proposed protocol. Moreover, a system of fixed and nomadic nodes was implemented to test the proposed localization algorithm. The reported experiments show a mean positioning error of 0.61 m and a mean orientation error of 17 degrees within a 10 m x 10 m square space.**

***Keywords*-Wireless Sensor Network; Energy Efficient Protocol; Differential Direction of Arrival; Switched Beam Antenna.**

I. INTRODUCTION

The management of mobility within Wireless Sensor Networks [1] (WSNs) has recently gained much interest as the number of applications that require nomadic sensor nodes has increased. The presence of nomadic nodes within a WSN allows the improvement of system monitoring capabilities but, at the same time, it increases the system complexity (since a localization algorithm is required), the energy consumption, as well as the delay and the latency of the network. For this purpose, adopting a nomadic WSN is expected to satisfy calls for a carefully localization algorithm and an optimized communication protocol able not only to minimize the energy waste, but also to synchronize the fixed and the nomadic nodes and to manage the localization procedure.

This paper deals with a communication and localization framework suitable for Nomadic WSN. In particular, after a brief description of the 2D Music algorithm, the proposed localization algorithm is presented in in Section III. In Section IV, the communication protocol is described. Finally, in Sections V and VI, protocol performance and some localization tests are reported.

II. 2-D MUSIC ALGORITHM

Let an array of N omnidirectional elements receive signals from L ($L < N$) narrowband far-field sources with the unknown Direction of Arrivals (DOAs) $\{\phi_1, \ldots, \phi_L\}$. The array $N \times 1$ snapshot vector at time k can be modeled as [2]

$$x(k) = A(\phi)s(k) + n(k) \tag{1}$$

where $\phi = [\phi_1, \ldots, \phi_L]^T$ is the $L \times 1$ vector of signal DOAs,

$$A(\phi) \doteq [a(\phi_1), \ldots, a(\phi_L)] \tag{2}$$

is the $N \times L$ signal steering matrix, $s(k)$ is the $L \times 1$ vector of signal waveforms, $n(k)$ is the $N \times 1$ vector of noise and $(\cdot)^T$ stands for the transpose.

Assuming an array of arbitrary geometry, the $N \times 1$ steering vector can be expressed as

$$a(\phi) = \left[\ldots, e^{j\frac{2\pi}{\lambda}(x_i sin\phi + y_i cos\phi)}, \ldots\right]^T \tag{3}$$

where λ is the signal wavelength, $j = \sqrt{-1}$, $\{x_i, y_i\}$ ($i = 1, \ldots, N$) are the coordinates of the ith array element and and it will be hereafter assumed that the array manifold is known exactly.

The $N \times N$ array covariance matrix can be written as

$$R_x \doteq E\{x(k)x^H(k)\} = AR_sA^H + \sigma_n^2 I \tag{4}$$

where $R_s = E\{s(k)s^H(k)\}$ is the source covariance matrix, σ_n^2 is the noise variance, I is the identity matrix, $E(\cdot)$ is the statistical expectation and $(\cdot)^H$ is the Hermitian transpose (transpose and conjugate of $(\cdot)$).

The singular value decomposition of the exact covariance matrix can be written as

$$R_x = \sum_{k=1}^{N} \lambda_k u_k u_k^H \tag{5}$$

where λ_k and u_k ($k = 1, \ldots, N$) are the singular values and corresponding singular vectors. Let the singular values λ_k be sorted in nonascending order. Then, the matrices

$$U_s \doteq [u_1, \cdots, u_L], \qquad U_n \doteq [u_{L+1}, \cdots, u_N] \tag{6}$$

 ISBN: 978-1-61208-231-8

contain L the signal and $N - L$ noise subspace singular vectors, respectively.

In practical situations, the exact array covariance matrix R_x is unavailable and its sample estimate

$$\hat{R}_x = \frac{1}{K} \sum_{k=1}^{K} x(k) x^H(k) \tag{7}$$

is used, where K is the number of snapshots.

The singular value decomposition of the sample covariance matrix (7) yields

$$\hat{R}_x = \hat{U}_s \hat{\Lambda}_s \hat{U}_s^H + \hat{U}_n \hat{\Lambda}_n \hat{U}_n^H \tag{8}$$

where the sample singular values are again sorted in nonascending order ($\hat{\lambda}_1 \geq \hat{\lambda}_2 \geq \cdots \geq \hat{\lambda}_N$) and the matrices $\hat{U}_s \doteq [\hat{u}_1, \ldots, \hat{u}_L]$ and $\hat{U}_n \doteq [\hat{u}_{L+1}, \ldots, \hat{u}_N]$ contain in their columns the signal and noise subspace singular vectors of $\hat{R}_x$, respectively. Correspondingly, the diagonal matrices $\hat{\Lambda}_s \doteq diag\{\hat{\lambda}_1, \ldots, \hat{\lambda}_L\}$ and $\hat{\Lambda}_n \doteq diag\{\hat{\lambda}_{L+1}, \ldots, \hat{\lambda}_N\}$ are built from the signal and noise subspace singular values of $\hat{R}_x$, respectively.

The conventional MUSIC null-spectrum function can be expressed as

$$f(\phi) = a^H(\phi) \hat{U}_n \hat{U}_n^H a(\phi) = \|\hat{U}_n^H a(\phi)\|^2 \tag{9}$$

where $\| \cdot \|^2$ is the vector 2-norm. The spectral MUSIC technique estimates the signal DOAs from the minima of this function by searching over ϕ with a fine grid. The computational complexity of this spectral search step is typically substantially higher than that of the singular value decomposition step because, as a rule, $J \gg N$ where J is the total number of spectral points. Note that for each spectral point, the product of $\hat{U}_n^H$ and $a(\phi)$ (or, alternatively of $\hat{U}_s$ and $a(\phi)$) has to be computed.

Often, the inverse of the normalized MUSIC null-spectrum function is considered to compute and exalt the signal DOAs. This function is computed as follow.

$$f(\phi) = \frac{\|a(\phi)\|}{\|\hat{U}_n^H a(\phi)\|^2} \tag{10}$$

In this case the signal DOAs is estimated from the maxima of (10).

III. Localization Algorithm

Let A, B and C be three *fixed nodes* positioned in a Euclidean Geometry Plane Π and having coordinates (x_A, y_A), (x_B, y_B) and (x_C, y_C), respectively.

Let M be a *nomadic node* also positioned in the plane Π and having generic coordinates (x_M, y_M). M is equipped by a Switched Beam Antenna characterized by a group of N directive antennas that together cover an angle of 360°. Let $a_i(\phi)$ $(i = 1, \ldots, N)$ be the azimuth steering vector (gain vector) of each directive antenna.

M computes its coordinates (x_M, y_M) in three steps.

1) It applies the MUSIC algorithm.
2) It applies the law of sines starting from the knowledge of the coordinates of the fixed nodes.
3) It performs the trilateration algorithm.

A. MUSIC algorithm

According to (1) and (7), M builds up for each fixed nodes K vectors of $N \times 1$ RSSI values. Let $x_{k0_i}(\cdot)$ $(k0 \in [1; K])$ the k^{th} RSSI vector of the fixed node i $(i = A, B, C)$. The position $x_{k0_i}(n0)$ $(n0 \in [1; N] \wedge k0 \in [1; K])$ will contain the RSSI value computed at the k^{th} iteration selecting the n^{th} antenna's sector. The RSSI values can also be organized in matrix form as follow.

$$X_i = \begin{pmatrix} x_{11_i} & \cdots & x_{1K_i} \\ x_{21_i} & \cdots & x_{2K_i} \\ \vdots & \ddots & \vdots \\ x_{N1_i} & \cdots & x_{NK_i} \end{pmatrix} \tag{11}$$

Then, according to (7) and (8), M computes for each fixed node the covariance matrix R_{x_i} $(i = A, B, C)$ as

$$\begin{aligned} R_{x_i} &= \tfrac{1}{K} \sum_{k=1}^{K} x_{k_i}(n) x_{k_i}^H(n) \\ &= U_{s_i} \Lambda_{s_i} U_{s_i}^H + U_{n_i} \Lambda_{n_i} U_{n_i}^H \end{aligned} \tag{12}$$

Finally, according to (10), M evaluates the angles ϕ_i $(i = A, B, C)$ as

$$\phi_i = argmax_\phi \frac{a(\phi)}{a^t(\phi) U_{n_i} U_{n_i}^t a(\phi)} \tag{13}$$

B. Law of Sine

Let a, b and c be the lengths of the legs of a triangle opposite angles $\hat{A}$, $\hat{B}$ and $\hat{C}$. Then the law of sines states that

$$\frac{a}{\sin \hat{A}} = \frac{b}{\sin \hat{B}} = \frac{c}{\sin \hat{C}}$$

If two sides of a triangle are the radius, the law of sines states that

$$|\overline{AB}| = 2R \sin(\frac{\phi_C}{2}) \tag{14}$$

where, as Figure 1 shows, $\overline{AB}$ is a chord, R is the radius of the circle and finally ϕ_C is the angle at the centre subtended by the chord $\overline{AB}$. Knowing also that:

1) angles at the circumnference subtended by a chord in the same segment are equal and
2) if two angles stand on the same chord, then the angle at the centre is twice the angle at the circumnference,

Equation (14) can be expressed as

$$|\overline{AB}| = 2R \sin(\phi_{AB}) \tag{15}$$

The law of sines is used by the nomadic node M to perform another step towards the evaluation of its position. From the knowledge of the coordinates of the anchor nodes

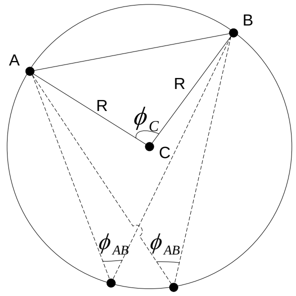

Figure 1: Specific application of law of sines

and the angles ϕ_A, ϕ_B and ϕ_C, M obtains the equation of three circumferences $\mathcal{A}$, $\mathcal{B}$ and $\mathcal{C}$ passing for M and for A and B, B and C and C and A, rispectively. The equations can be expressed as follow:

$$\begin{aligned}
\mathcal{A}: &\quad (x - x_{\mathcal{A}})^2 + (y - y_{\mathcal{A}})^2 = \tfrac{(x_B - x_A)^2 + (y_B - y_A)^2}{2\sin\hat{\phi}_{AB}} \\
\mathcal{B}: &\quad (x - x_{\mathcal{B}})^2 + (y - y_{\mathcal{B}})^2 = \tfrac{(x_C - x_B)^2 + (y_C - y_B)^2}{2\sin\hat{\phi}_{BC}} \\
\mathcal{C}: &\quad (x - x_{\mathcal{C}})^2 + (y - y_{\mathcal{C}})^2 = \tfrac{(x_A - x_C)^2 + (y_A - y_C)^2}{2\sin\hat{\phi}_{CA}}
\end{aligned}$$

where

$$\begin{aligned}
(x_{\mathcal{A}}, y_{\mathcal{A}}) &= \tfrac{1}{2}(x_A + x_B, y_A + y_B) + \\
&+ \tfrac{1}{2}(y_A - y_B, -x_A + x_B)\cot\hat{\phi}_{AB} \\
(x_{\mathcal{B}}, y_{\mathcal{B}}) &= \tfrac{1}{2}(x_B + x_C, y_B + y_C) + \\
&+ \tfrac{1}{2}(y_B - y_C, -x_B + x_C)\cot\hat{\phi}_{BC} \\
(x_{\mathcal{C}}, y_{\mathcal{C}}) &= \tfrac{1}{2}(x_C + x_A, y_C + y_A) + \\
&+ \tfrac{1}{2}(y_C - y_A, -x_C + x_A)\cot\hat{\phi}_{CA}
\end{aligned}$$

are the centers of the circles and $\hat{\phi}_{AB}$, $\hat{\phi}_{BC}$ and $\hat{\phi}_{CA}$ are $\hat{\phi}_A - \hat{\phi}_B$, $\hat{\phi}_B - \hat{\phi}_C$ and $\hat{\phi}_C - \hat{\phi}_A$.

C. Trilateration Algorithm

Finally, M finds its position performing the trilateration. In particular, it finds the intersection point of the cirmunferences $\mathcal{A}$, $\mathcal{B}$ and $\mathcal{C}$. This concept is shown in Figure 2.

The intersection point is simple to compute thanks to the following formulas:

$$\begin{aligned}
x &= x_{\mathcal{A}} + \tfrac{d_x k}{p} + \tfrac{d_y}{p}\sqrt{r_{\mathcal{A}}^2 - k^2} \\
y &= y_{\mathcal{A}} + \tfrac{d_y k}{p} - \tfrac{d_x}{p}\sqrt{r_{\mathcal{A}}^2 - k^2}
\end{aligned}$$

where $d_x = x_{\mathcal{A}} - x_{\mathcal{B}}$, $d_y = y_{\mathcal{A}} - y_{\mathcal{B}}$, $p = \sqrt{d_x^2 + d_y^2}$ and $k = \frac{p^2 + r_{\mathcal{A}}^2 - r_{\mathcal{B}}^2}{2p}$.

Once the position of the nomadic node is estimated, the orientation is determined in a straigh-forward manner. Given the position, the angle between the nomadic node and one of the anchor is easily derived as

$$\theta_B = \frac{x_M - x_B}{y_M - y_B}$$

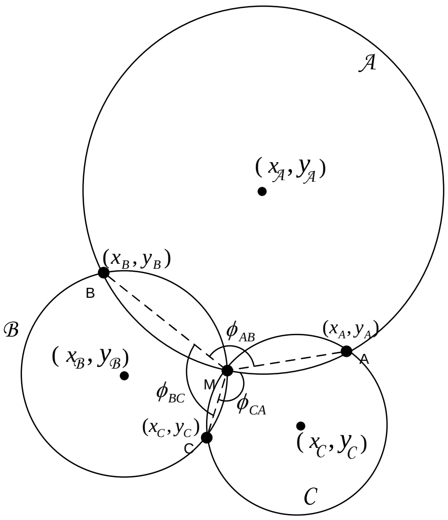

Figure 2: Trilateration

The nomadic node orientation is simply estimated as

$$\psi = \theta_B - \phi_B$$

IV. MAC Protocol

Taking the IEEE 802.11 Distributed Coordination Function (DCF) [3] as a starting point, several more energy efficient techniques have been proposed in literature to avoid excessive power waste due to so called idle listening. They are based on periodical preamble sampling performed at the receiver side in order to leave a low power state and receive the incoming messages, as in the WiseMAC protocol [4]. Deriving from the classical contention-based scheme, several protocols (S-MAC [5] and TMAC) have been proposed to address the overhead idle listening by synchronizing the nodes and implementing a duty cycle within each slot.

Resorting to the above considerations, a class of MAC protocols was derived, named *Synchronous Transmission Asynchronous Reception* (STAR) which is particularly suited for a flat network topology and benefits from both WiseMAC and S-MAC schemes. More specifically, due to the introduction of a duty-cycle, it joins the power saving capability together with the advantages provided by the offset scheduling, without excessive overhead signaling.

According to STAR protocol, each node wakes up independently, entering an initial idle state (*init state*) in which it remains for the time interval necessary for performing the elementary CPU operations and to be completely switched on (T_{init}). Moreover, before entering the *discovery state*, each device starts to organize the time into frames whose durations are T_f.

In the *discovery state*, each node tries to identify its neighbors and to establish a time synchronization with them. To this purpose, it remains in a listening mode for a time interval equal to $T_{set-up} \geq 2T_f$ and begins to periodically broadcast a HELLO message sending its *ID* and its *phase*. The phase is the time interval after which the sender exits from the *discovery state*, enters the regime state and changes back in listening mode. A node that receives a HELLO message adds the source node to the list of its own active neighbors and transmits an acknowledgement.

Once the *discovery state* has expired, each node enters the *regime state*. Within this state, the operation mode is duty cycled with a periodic alternation of listening and sleeping sub-periods whose time intervals are T_l and T_s, respectively. The duty cycle function is given by the following formula:

$$d = \frac{T_l}{T_l + T_s} \tag{16}$$

In the *regime state*, each node tries to preserve the synchronization with its neighbors. To achieve this, it sends a frame-by-frame HELLO message in a unicast way to the active nodes in its list according to the phase transmitted by them in previous HELLO messages. As in the *discovery state*, the HELLO message contains the *ID* and the *phase* that, in this case, is the time interval after which the sender claims to be again in the listening status waiting for the HELLO messages. The phase ϕ is evaluated according to the following rule:

$$\phi_1 = \tau - T_l \tag{17}$$

if the node is in the sleeping mode, where τ is the time remaining to the beginning of the next frame. Conversely, if the node is in the listening status, ϕ_2 is computed as:

$$\phi_2 = \tau + T_s \tag{18}$$

In the *regime state*, nomadic nodes are able to move within the operative area. Unlike the fixed nodes equipped by an omnidirectional antenna, they are hardwired with a *Switched Beam Antenna*, a group of N overlapping adjacent beams (sectors) that together cover an angle of $360°$. When a nomadic node reaches its intermediate waypoint, it stops for a predefined pause time (T_{pt}) and broadcasts a HELLO message per sector for a time interval equal to $2T_f$ by notifying its presence and listening the channel in search of HELLO messages sent by the fixed nodes in its coverage area. At the end of the scanning, if the nomadic node found a number of active fixed nodes less than three, it moves itself; otherwise it groups the fixed nodes per sector and chooses the three nodes with the hightest RSSI value and belonging to different sectors (preferably opposite sectors). If this choice is not possible, it takes into account only the three nodes with the hightest RSSI value.

According to the *phase* stored during the scanning interval, the nomadic node sends a LOCALIZATION REQUEST message to the first fixed node. The fixed node wakes up and sends k ($k/N \in \mathbb{N}^+$) LOCALIZATION RESPONSE messages thanks to which the nomadic node creates a $k/N \times N$ matrix of RSSI values.

The nomadic node performs the same procedure to the other two fixed nodes.

Finally, it applies the localization algorithm described in Section III to evaluate its position within the operative area.

Once T_{pt} is expired, it keeps moving again.

The channel access is managed by means of the carrier sense multiple access with collision avoidance (CSMA/CA) scheme. This mechanism is very effective in reducing collisions.

Each node remains in the *regime state* until there is at least one neighbor, otherwise if there are no active neighbors it reenters the *discovery state* in search of connectivity.

To complete the protocol characterization, whenever a node battery is depleted, this node turns off, entering an *off state*.

V. Protocol Performance Analysis

In order to fully characterize the STAR MAC approach, the related energy cost normalized can be evaluated, as follows:

$$C = c_{rx} d T_f + c_{sleep}[T_f(1-d) - NT_{pkt}] + NC_{tx} \quad [mAh] \tag{19}$$

where c_{sleep} and c_{rx} represent the sleeping and the receiving costs $[mA]$ and C_{tx} is the single packet transmission costs $[mAh]$, T_f is the frame interval $[s]$, d is the duty cycle, T_{pkt} is the synchronization packet time length $[s]$ and finally N is the number of neighbors. When the following inequality holds:

$$NT_{pkt} \ll T_f \tag{20}$$

then:

$$C \simeq c_{rx} d T_f + c_{sleep} T_f (1-d) + NC_{tx} \quad [mAh] \tag{21}$$

The protocol cost normalized to the synchronization time is finally:

$$\frac{C}{T_f} = c_{rx} d + c_{sleep}(1-d) + \frac{NC_{tx}}{Tf} \quad [mA] \tag{22}$$

As highlighted in TABLE I, it usually happens that $c_{tx} \ll c_{sleep} \ll c_{rx}$, where $c_{tx} = C_{tx}/T_{pkt}$ and T_{pkt} is the packet transmission time $[s]$ assumed equal to $100\ ms$ as worst case. This means that the major contribution to the overall cost is represented by the listening period that the STAR MAC protocol tries to suitably minimize.

TABLE I: POWER CONSUMPTION PARAMETERS FOR THE CONSIDERED PLATFORM

c_{rx}	12 mA
c_{sleep}	0.01 mA
C_{tx}	30 mAh
c_{tx}	0.001 mA

In Figure 3(a), the normalized cost versus the number of neighbor nodes is shown for the S-MAC and STAR

MAC schemes. It is worth noticing that the performance of the proposed protocol is better with respect to the existing approach for a number of neighbor nodes greater than 7. In Figure 3(b), the normalized costs of S-MAC and STAR MAC approaches are compared with respect to the duty cycle duration for a number of neighbor nodes equal to 8. It is possible to notice that for $d < 3.5\%$ the proposed protocol provide a significant gain.

VI. Experimental Localization Results

In this section, some experimental results are presented.

The experiments were conducted in a room of $10m \times 10m$. Fixed nodes assumed the following positions: $A = (1.25, 1.78)$ m, $B = (8.66, 1.81)$ m and $C = (4.50, 8.50)$ m, respectively. This arrangement resambles an almost equilateral triangle, a suited shape to uniformly covers the test area. Otherwise nomadic node assumed four position $P_1 = (4.50, 4.72)$; $P_2 = (2.85, 4.72)$, $P_3 = (6.20, 4.72)$, $P4 = (4.50, 5.50)$. The nomadic node reference was always parallel to the positive x axis, i.e it faces the east direction.

Both fixed and nomadic nodes were able to scan signals in a emphomnidirectional manner (in a 2D sense), but in a different sense. The fixed nodes were equipped with a common dipole, a standard low-gain omnidirectional radiator. The nomadic node instead was equipped with a Switched Beam Antenna (SBA).

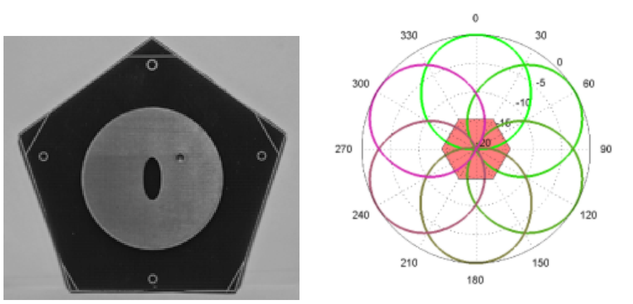

(a) Antenna Element (b) Pictorial Representation of the 6 Patterns

Figure 4: Switching beam system. Given the antenna pattern, a six elements arrangement is enough to cover the entire angular range.

To keep a cost-effective profile, this array is made of 6 printed antennas working at 2.45 GHz directly fed by a commercial single pole six through (SP6T) FET switch. The natural arrangement to cover the entire 2π angular range is the uniform circular array (UCA). This structure is the best trade-off between the need of simple architecture for and a wide angle steerable beam. The SBA gain G can be represented by six element vectors. This structure is the best trade-off between the need of a simple architecture and a wide angle steerable beam. The elementary patch antenna of the array shown in Figure 4 is an Elliptical Slitted Disc Antenna [6], a circularly polarized radiator well suited for localization purposes. Printed on a cheap plastic substrate ($\varepsilon_r = 4.4$, $h = 1.6$ mm), the antenna shows a cardioid-like pattern, suitable for the switched beam arrangement. The compact dimension of 35 mm is a good compromise between CP radiations and pattern degradation by electromagnetic coupling.

The results of the four experiments are depicted in Figure 5 and Figure 6. In all the cases, the radial error was below 90 cm, and the orientation of the system was identified within the $35°$ of pointing error. The entire experimental data set showed an average error in the position estimation of 0.61 m and $17°$ for the orientation.

VII. Conclusion and Future Work

The management of mobility within WSNs has recently gained much interest as the number of applications that require nomadic sensor nodes has increased. The presence of nomadic nodes within a WSN allows the improvement of system monitoring capabilities but, at the same time, it increases the system complexity (since a localization algorithm is required), the energy consumption, as well as the delay and the latency of the network.

In this paper, a communication and localization framework was proposed. The numerical and experimental results showed the advantages and the feasibility of the proposed solution. This allows the application of the solution under investigation to the more general field of environmental monitoring and in particular in robot applications.

Acknowledgment

The authors would like to thank T.T. Tecnosistemi S.p.A.

References

[1] J. Yick, B. Mukherjee and D. Ghosal, *Wireless sensor network survey*, in Journal on Computer Network, Vol. 52, pp. 2292-2330, April 2008.

[2] R.O. Schmidt, *Multiple Emitter Location and Signal Parameter Estimation*, in IEEE Transaction on Antennas and Propagation, Vol. 34, pp. 276-280, March 1979.

[3] I. of Electrical and E. Engineers, *Wireless LAN Medium Access Control (MAC) and Physical Layer (PHY) Specifications*, IEEE Standard 802.11-1997, New York, NY, 1997.

[4] A. El-Hoiydi, J. Decotignie, C. Enz, and E. Le Roux, *WiseMAC, an Ultra Low Power MAC Protocol for the WiseNET Wireless Sensor Network*, in Proc. of SENSYS 2003, Vol. 1, pp. 244-251, November 2003.

[5] W. Ye, J. Heidemann, and D. Estrin, *An Energy-Efficient MAC Protocol for Wireless Sensor Networks*, in Proc. of INFOCOM 2002, vol. 3, pp. 1567-1576 June 2002.

[6] S. Maddio, A. Cidronali and G. Manes, *A New Design Method for Single-Feed Circular Polarization Microstrip Antenna with an Arbitrary Impedance Matching Condition*, in IEEE Transactions on Antennas and Propagation, 2010.

 ISBN: 978-1-61208-231-8

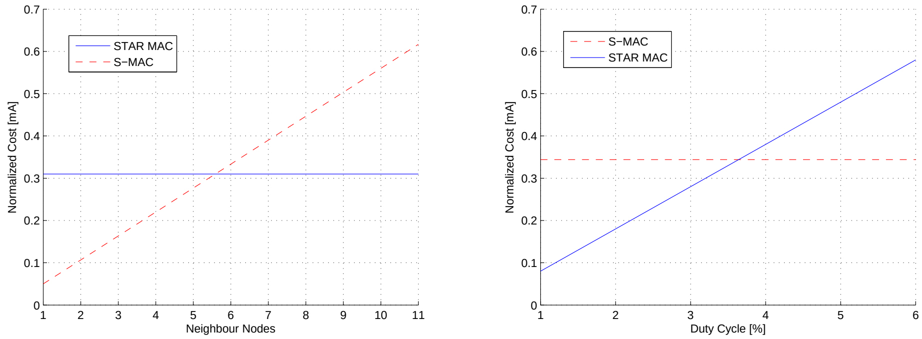

(a) Normalized Cost vs. Neighbor Nodes

(b) Normalized Cost vs. Duty Cycle Duration

Figure 3: STAR MAC Performance

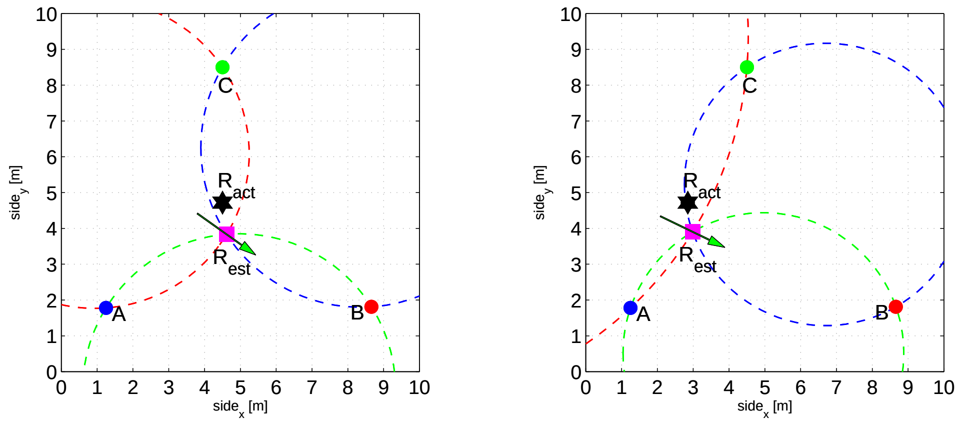

(a) experiment #1: actual position: $(\hat{x}, \hat{y}) = (4.50, 4.72)$, $err_{xy} = (0.11, -0.88)$, $err_{tot} = 0.89$, $ori_{err} = -35$

(b) experiment #2: actual position: $(\hat{x}, \hat{y}) = (2.85, 4.72)$, $err_{xy} = (0.13, -0.81)$, $err_{tot} = 0.82$, $ori_{err} = -25$

Figure 5: The first two experiments. The hexa-star is the actual position of the nomadic node (indicated with R), while the square is the estimated position and arrow indicates the estimated orientation.

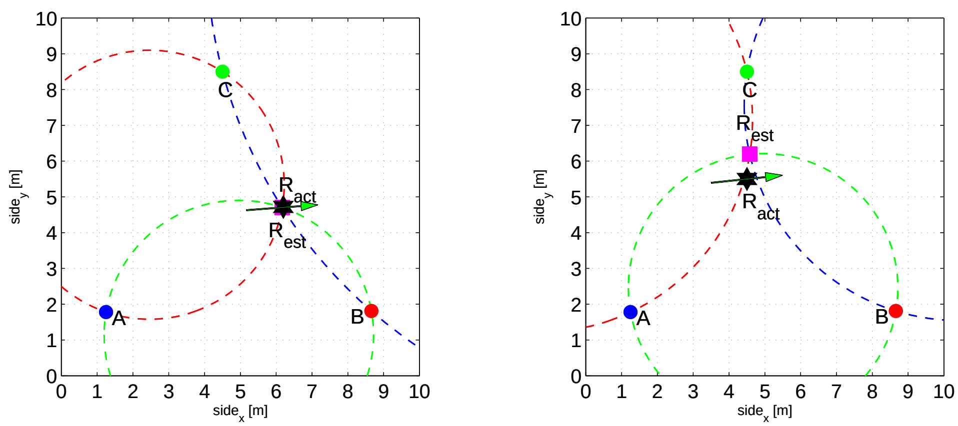

(a) experiment #3: actual position: $(\hat{x}, \hat{y}) = (6.20, 4.72)$, $err_{xy} = (-0.03, -0.01)$, $err_{tot} = 0.03$, $ori_{err} = 4$

(b) experiment #4: actual position: $(\hat{x}, \hat{y}) = (4.50, 5.50)$, $err_{xy} = (0.08, 0.69)$, $err_{tot} = 0.69$, $ori_{err} = 6$

Figure 6: The second two experiments. The hexa-star is the actual position of the nomadic node (indicated with R), while the square is the estimated position and arrow indicates the estimated orientation.

 ISBN: 978-1-61208-231-8